Mulakkal, M. C., Seddon, A. M., Whittell, G., Manners, I., & Trask, R. S. (2016). 4D fibrous materials: Characterising the deployment of paper architectures. *Smart Materials and Structures*, *25*(9), [095052]. https://doi.org/10.1088/0964-1726/25/9/095052

Peer reviewed version

4D FIBROUS MATERIALS: CHARACTERISING THE DEPLOYMENT OF PAPER ARCHITECTURES

Manu C Mulakkal[1], Annela M. Seddon[2,3], George Whittell[4], Ian Manners[4] and Richard S. Trask[5]

[1]Advanced Composites Centre for Innovation and Science (ACCIS), Department of Aerospace Engineering, University of Bristol, Bristol, BS8 1TR, UK

[2]School of Physics, HH Wills Physics Laboratory, Tyndall Avenue, University of Bristol, Bristol, BS8 1TL, UK

[3]Bristol Centre for Functional Nanomaterials, HH Wills Physics Laboratory, Tyndall Avenue, University of Bristol, Bristol, BS8 1TL, UK

[4]School of Chemistry, Cantock's Close, University of Bristol, Bristol, BS8 1TS, UK

[5]Department of Mechanical Engineering, University of Bath, Bath, BA2 7AY, UK

Abstract

Deployment of folded paper architecture using a fluid medium as the morphing stimulus presents a simple and inexpensive methodology capable of self-actuation; where the underlying principles can be translated to develop smart fibrous materials capable of programmable actuations. In this study we characterise different paper architectures and their stimuli mechanisms for folded deployment; including the influence of porosity, moisture, surfactant concentration, temperature, and hornification. We observe that actuation time decreases with paper grammage; through the addition of surfactants, and when the temperature is increased at the fluid-vapour interface. There is a clear effect of hydration, water transport and the interaction of hydrogen bonds within the fibrous architecture which drives the deployment of the folded regions. The importance of fibre volume fraction and functional fillers in shape recovery was also observed, as well as the effect of a multilayer composite paper system. The design guidelines shown here will inform the development of synthetic fibrous actuators for repeated deployment.

Key words: 4D materials, composite morphing, origami, self-actuation

1 Introduction

The medium of paper has been used as a material since its invention in Ancient China during the Han dynasty (206BC-220AD), and remains in common practice due to its ease of large scale production and low cost. However, whilst functioning as a simple two-dimensional sheet, it has been shown since the 6th Century that paper is capable of being utilised as a three-dimensional building material. The Japanese art of origami (which literally translates as "to fold paper") and associated techniques such as Kirigami (from the Japanese "to cut paper"), and more pertinent to this work, "wet folding" origami have been used decoratively, but also as the inspiration for modern materials design. Origami and Kirigami maximise the potential of traditional folding processes (i.e. mountain and valley folds) in realising complicated geometries capable of morphing through bi-stable or multi-stable configurations, through the employment of low activation energies.

Multi-material self-actuating synthetic systems, with inherent active and passive regions transforming through origami folding, have been reported in the literature for different stimuli methods; for example, employing polymer swelling and shrinking [1]; shape-memory materials [2] and magnetic materials [3]. Among polymers, hydrogels in particular have received a great deal of attention in the research community due to their large homogeneous volumetric change. To date numerous stimulus have been reported in the open literature; such as water, light (photoactive), temperature, pH, electric field, specific solvent and enzymes have been reported [4–6]. Their swelling response is similar to biological cytoplasm, triggering research to develop artificial muscles [7]. By restricting the homogenous swelling (or shrinking) of the

polymer network (i.e. through electrically embedding ions, i.e. ionoprinting [8]), promotes inhomogeneous changes which can be programmed for controlled folding or bending patterns of the polymer membrane [9].

The components of paper itself, have been studied as a self-actuating material; for example, the hygroscopic swelling of a bi-layer natural cellulose composite (based on Timoshenko's research on bimetallic strips [10]) to develop self-actuating components triggered by the swelling differential across neighbouring layers. Similar, to the bi-metallic strip, the cellulose bi-layer design results in a bending moment to accommodate the through-thickness induced strain in the material [11]. This approach has been reported for paper-plastic[12] and wood veneer-glass epoxy composites[13]. However, understanding and controlling the underlying principles of deployment of cellulose-based architectures is still not well understood. By way of example, the work by Etienne Cliquet in his Flotilla art exhibition [14], shows the unfolding deployment of multiple paper origami folds once in contact with water. Unlike the aforementioned bi-layer natural and synthetic systems, this material lacks any distinct active or passive layers, or layered architecture as observed in pine cones[3] and wheat awns[15–17] controlling the Poison's effect, and yet still deploys in a timely fashion without the complexity of previous work. Understanding the science behind this deployment permits the development of simplistic approaches for manufacturing complex architectures (from 2-dimensional membranes) and as an inherent programmed morphing mechanism for active shape change. This has direct relevance on the development of self-actuating functional materials as effective space saving solutions for deployable structures across a variety of length scales from microelectromechanical systems (MEMS) to heart stent to space-mast/ boom[18–20].

In this study we characterise the deployment mechanisms for different paper architectures leading to specific folding/unfolding design rules for future synthetic composite material systems. We consider the influence of porosity, moisture, surfactant concentration, temperature, and hornification in the deployment of sample architectures. Understanding, the role of the substrate, its architecture and the environmental stimulus is essential in generating the next generation of active 4-dimensional (4D) fibrous materials as internal actuators for morphing structures.

2 Characterisation of paper substrates

2.1 PAPER TYPE

A number of different commercial paper weight types, (usually referred to as grammage (gsm - grams/ square meter)), and origins were investigated to ascertain the effect of grammage, filler, and fibre type on the rate of deployment. In this study, the papers selected were; Printer paper (90 gsm) from Office Depot - A4 Advanced Laser Paper, handmade Lokta (60 gsm), handmade Lokta (30 gsm), and handmade Sekishu (30 gsm) from www.paperworks.uk.com.

Commercial printer paper is manufactured with the addition of fillers (such as Calcium carbonate, Kaolin, Talc and TiO_2 [21]) and sizing agents to improve the colour and ink absorption. Conversely, Lokta and Sekishu papers are handmade fine art papers made from the fibres of Lokta plant (*Daphne papyracea*) from Nepal and Kozo plant (*Broussonetia papyrifera*) from Sekishu region in Japan respectively. They are un-sized and lack any additional filler material.

Paper Microstructure

The physical architecture of each paper type was characterised by light microscopy (Zeiss AX10) and scanning electron microscopy (JSM-IT300). Figure 1 shows the significant differences in the microstructure and constituents across the 4 different samples. From these observations, the printer paper can be considered to be similar to synthetic structural composite materials; where the fibres act as the reinforcement phase with the filler material forming the surrounding supporting matrix. By comparison, the handmade paper essentially consists of a series of inter-connected short fibre bundles arranged in discrete layers. As the figure illustrates, the handmade papers have an open fibrous architure exhibiting excellent pore connectivity both intra-ply and inter-ply.

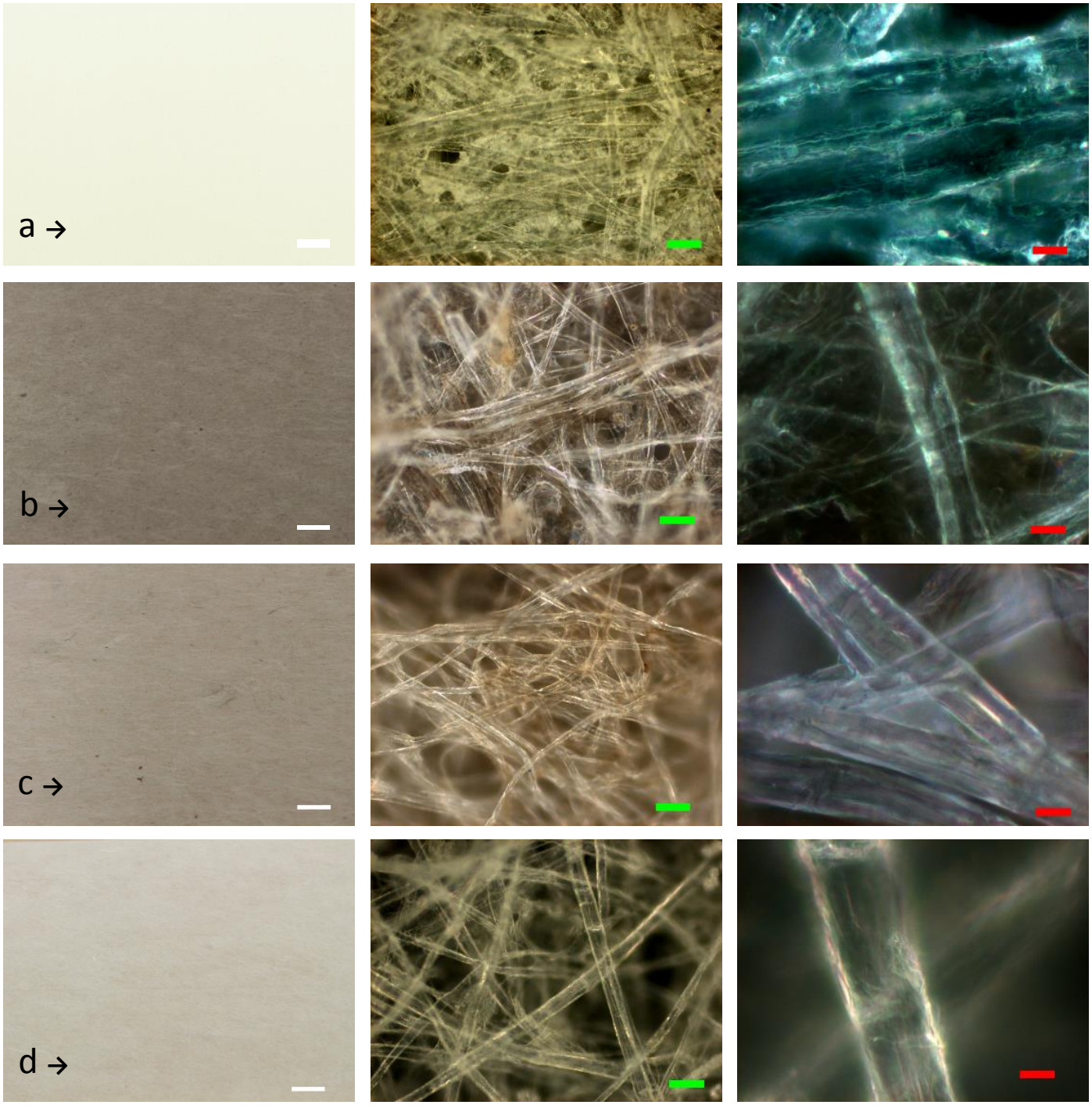

Figure 1: Optical microscopy a) Printer paper 90 gsm b) Lokta 60 gsm c) Lokta 30 gsm and d) Sekishu 30 gsm. (White scale bar = 10 mm; Green Scale bar = 50 µm; Red scale bar = 10 µm)

Contact Angle Measurements (CA)

To generate clear design guidelines concerning the specific folding/unfolding rules for future synthetic fibrous morphing material systems, we must first characterise and understand the role of the stimuli in our model system; namely, the fluid-surface and fluid-transport interaction. Clearly, the surface properties of the different paper types will greatly affect the fluid transport on the surface, and the transport mechanisms through into the bulk of the material. In order to quantify the 'wettability' of the surface, a series of contact angle measurements were performed using a Drop Shape Analyser (KRÜSS DSA 100).

Due to the inherent porosity and absorbing nature of the different paper substrates, a static assessment of CA was not possible in this work. However, in order to fully quantify the change in contact angle with time, a continuous assessment of droplet absorption over a set time period was undertaken. Figure 2 shows an average of five runs from various regions across two different samples of each paper type. Here, we only consider stable regions due to the absorbed droplet triggering swelling and out-of-plane deformation (wrinkles) of the substrate especially towards the end of complete absorption, leading to erroneous CA data results being recorded. The out-of-plane wrinkles were particularly disruptive on hand made paper specimens and resulted in erroneous high CA– it was noted that the water droplet was eventually absorbed by all substrates but the decay in the CA measurement was masked by the increase in swelling size of the substrate and wrinkles during hydration.

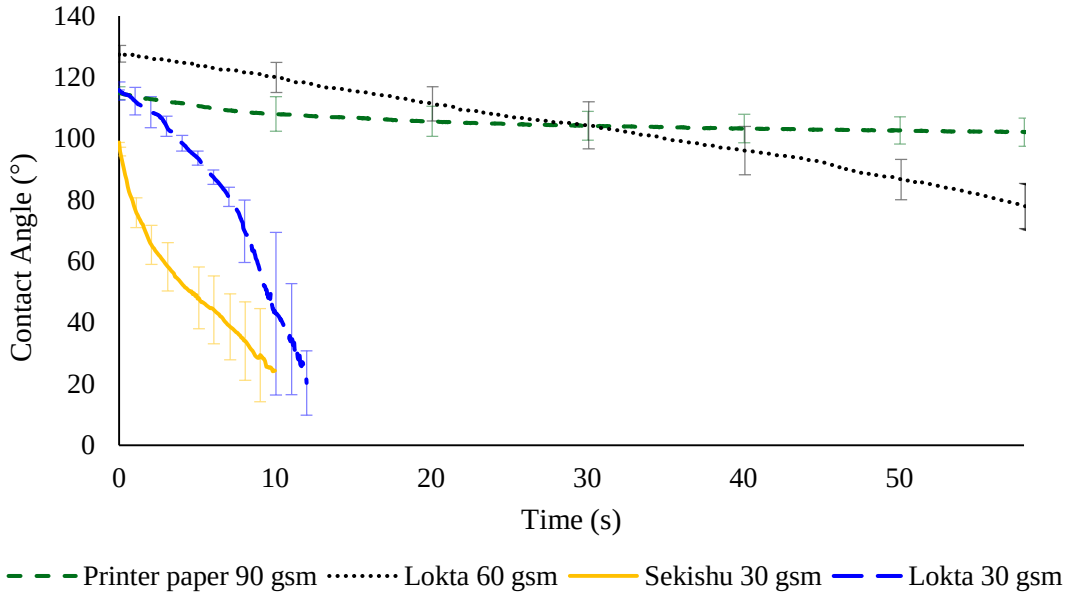

Figure 2: Stable CA of different paper types during droplet absorption as a function of time

The CA values at time (t) = 0 gives a comparative representation of factors such as roughness and surface chemistry, and thus wettability of the substrate. Whilst great care was undertaken to test similar specimens and regions of comparable volume fraction, the tortuosity of the surface profile under the droplet will strongly influence the initial CA values. This is evident in the recorded CA values for the Lokta 30 gsm and 60 gsm specimens, despite being produced from the same fibrous material. The change in CA with time reflects the absorption of water by the paper due to the internal microstructure and inherent porosity rather than the molecular composition of the substrate. The variation in microstructure (porosity) is considered to be the source of high standard deviation at the later stages of absorption. The fillers and sized fibres in printer paper resist the droplet absorption into the substrate, which is evidenced by the very small change in CA with time observed in printer paper.

2.2 SHAPE SELECTION

To consistently characterise the folding/unfolding behaviour of the different paper architectures, a model cross shape architecture (as shown in Figure 3) was chosen for evaluation; this geometrical shape simplifies the 'valley' fold creation, whilst also permitting the longitudinal and transverse 'arms' to be evaluated simultaneously (thus illustrating any fibre bias which might have occurred in the creation of the paper sheet). The profile dimensions were chosen so as to maximise the sample contact area with the fluid medium. The profile was generated in CAD, printed on A4 sheet of paper using a laser printer, and then extracted. For the handmade papers, the printed profiles were used as a stencil to extract samples. The extracted profile was then folded manually with three valley folds spaced 5mm apart in each 'leg'. The representative deployment sequence for a folded configuration is shown in Figure 3. The time taken to reveal the full profile from the folded shape was termed as actuation time. It was observed that natural drying (at room temperature,

21 °C) of the deployed samples resulted in partial shape recovery of the original folded architecture; especially for the printer paper 90 gsm samples (this is discussed in section 4).

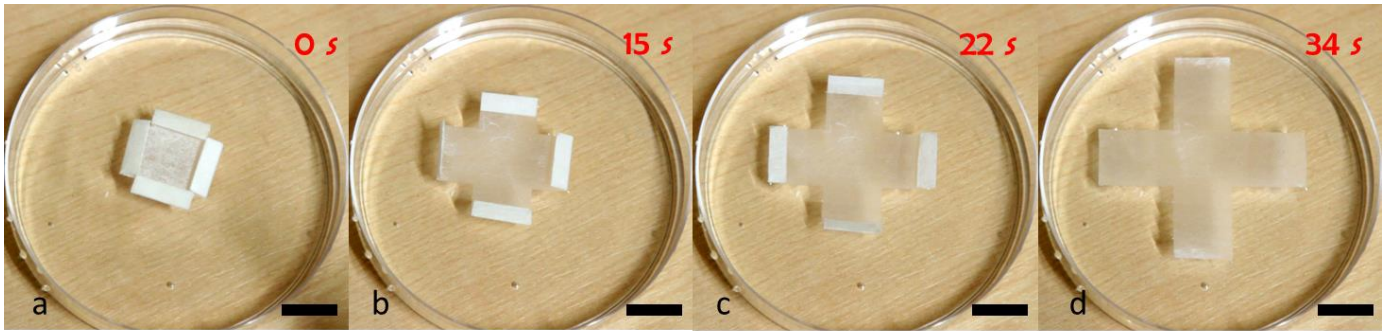

Figure 3: Deployment sequence (a-d) of the folded profile of Sekishu paper. Scale bar: 15 mm

2.3 CHARACTERISATION OF STIMULI

In order to ascertain the relationship between microstructural permeability and structural deployment, a number of liquid mediums was used to actuate the different paper architectures, namely water (the primary stimuli), oil (olive oil with a viscosity of approximately 100 cSt [22]) and alcohol (Methanol, Ethanol, and Glycerol). The results of these experiments are discussed in detail in the following sections.

Actuation media

A summary of deployment trials in different media is shown in Table 1.The average actuation time (from closed to fully deployed) in water for a minimum of 5 samples (per paper type) are presented in Table 1. The results indicate that printer paper took the longest to deploy to the full profile, and had greater standard deviation compared to other paper types. This variation was attributed to the non-uniform microstructure resulting from the paper manufacturing process; it is speculated that the chemical treatments and additional fillers to improve ink absorption and arrest discolouration inhibit the water ingression thus delaying the valley fold deployment. The very nature of this continuous manufacturing process means that the consistency can vary significantly, even in a single sheet of paper [23]. For example, a small difference in the time required to open the folds in the transverse and longitudinal 'legs' was observed for the 90 gsm printer paper; suggesting a bias in fibre direction due to processing method. Since this difference was minimal, the variation in actuation time as a result of fibre angle bias was not explored further.

It was observed that all the paper types could be deployed to some (partial) extent using a moist environment created using wet tissues in an enclosed chamber; in these environments it was noted that the actuation time was 2 orders of magnitude higher, i.e. Lokta 30 gsm deployed in approximately 2 hours in a moist room temperature environment and only took 30 seconds when placed in a water bath. This is clearly a function of the volume and rate of water required to permeate, react and soften the fibre architecture for deployment. Additionally, Methanol (99%), Ethanol (99%) and Olive Oil were evaluated but it was noted that whilst they completely wetted out the samples, none of these systems were capable of triggering the deployment sequence in any of the different paper architectures. Conversely, Glycerol did trigger a partial deployment sequence but only after specimen saturation had been attained (typically this took many hours). Table 1 pictorially summarises the final result/position of deployment trials for different liquid stimuli. The unfolding is triggered by the intraction of Hydrogen bonds in water and glycerol with the Hydrogen bonds in cellulose.

Table 1: Summary of paper type actuation in different liquid mediums at room temperature (25 °C)

	Printer paper	**Lokta 60**	**Lokta 30**	**Sekishu 30**
Water	Full deployment 313.1±152.4 s 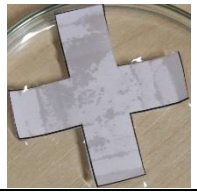	Full deployment 132±9.80 s 	Full deployment 25±4.47 s 	Full deployment 37.6±11.84 s 
Ethanol	sank without opening 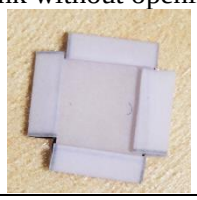	sank without opening 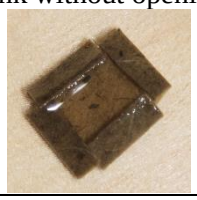	sank without opening 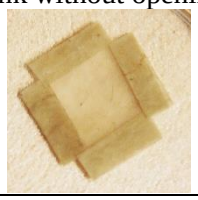	sank without opening 
Methanol	sank without opening 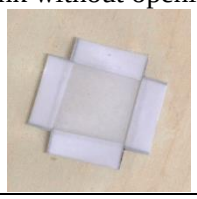	sank without opening 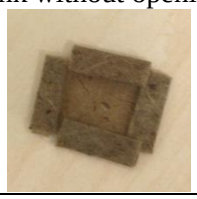	sank without opening 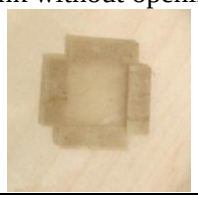	sank without opening 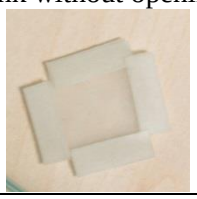
Olive Oil	sank without opening 	sank without opening 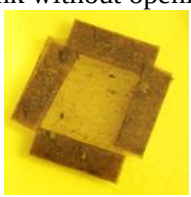	sank without opening 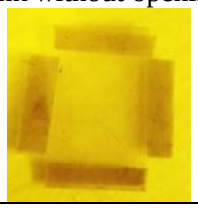	sank without opening 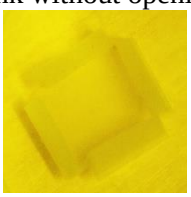
Glycerol	sank and partially opened over night 	sank and partially opened over night 	sank and partially opened (4 hrs) 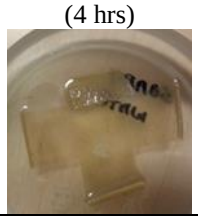	sank and partially opened (6 hrs) 

3 Fold Lines

Mountain and valley folds are key to achieving the packing efficiency in origami based architectures. In paper architectures, this involves permanently deforming the surface beyond its elastic limit. In origami terms, such folds are referred to as creases. From a structural point of view, this pre-stressing is likely to result in internal defects which would typically limit the usefulness of the structure. When folds are created in paper, one side undergoes extension whilst the other exhibits localised compressive deformation. Understanding the nature and magnitude of the internal damage, and its role on the deployment kinetics, is essential in the design of multi-deployable architectures.

Examination of the folded region revealed that the fibres are not torn when the folds are created but deform and re-position themselves to minimise the local strain field. In the case of printer paper, cracks are developed in the brittle filler materials since it is unable to cope with the localised strain of folding. These cracks then serve as a low resistance flow path for penetrating liquids as shown in Figure 4 *top row (a-c)*. Water coloured with food dye was used here for improved visualisation. The fold line can withstand high local strains without failure due to a number of local and global features. It is hypothesized that the overlapping fibre network (seen in Figure 1) provides pseudo-ductility by rearranging

the local architecture to absorb the global energy of folding. Furthermore, the stretching and/ or twisting of micro-fibrils on nano scale provides flexibility to the individual fibres. The formation of localised delamination between layers during the folding process is another means of energy dissipation. These mechanisms operating on a nano, micro and macro level ensure that the fibres can withstand the sharp folds without premature failure. Unlike synthetic man-made composites which rely on interfacial chemical bonding, in paper the individual layers are held by means of hydrogen bonds which offer reversible adhesion by hydration and dehydration.

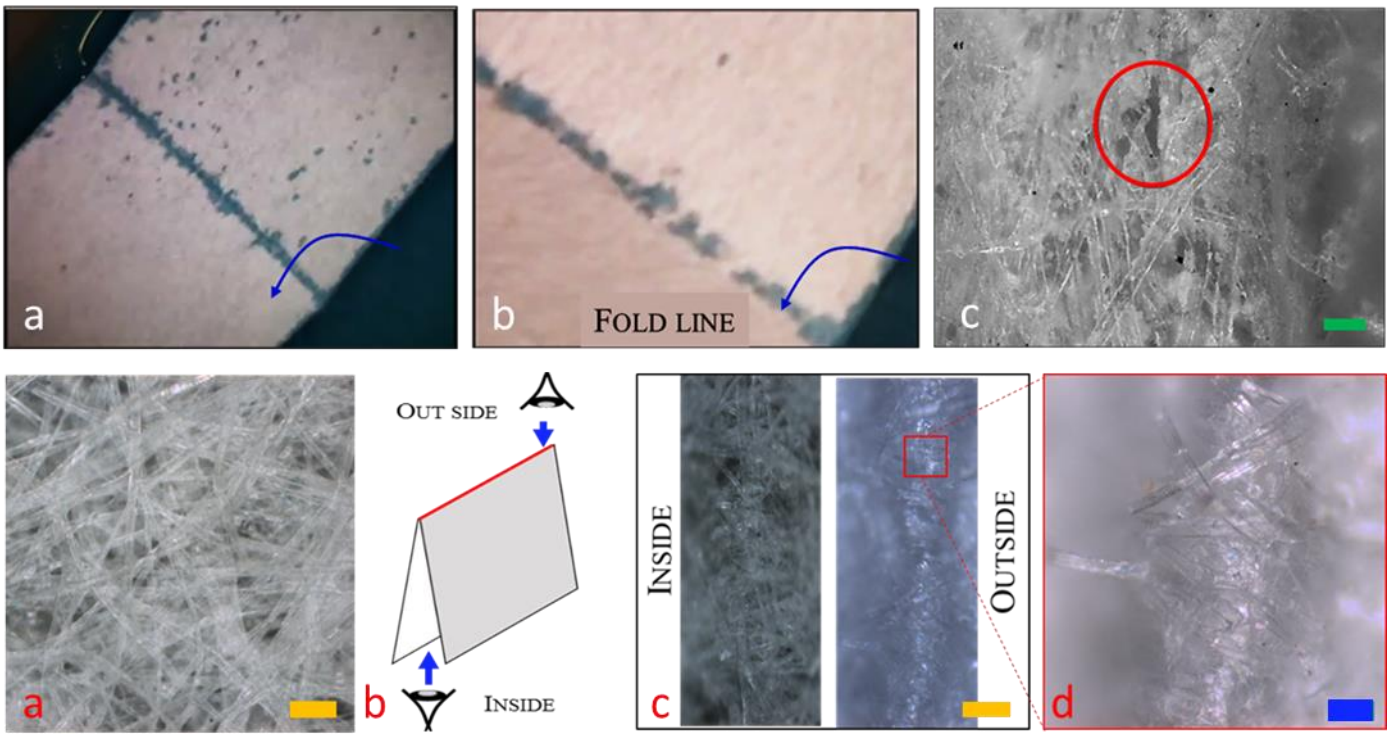

Figure 4: *Top row*: Printer paper 90 gsm a) Development of low resistance flow paths b) Close up view. Blue arrows indicate deployment direction c) Cracks formed in printer paper; *Bottom row*: Sekishu 30 gsm a) Before folding b) Fold scheme c) Fold-line visualisation d) close up of outside of the fold line (Green scale bar = 20µm , Gold scale bar = 100 µm and Blue scale bar = 50µm)

It is the unique ability of the random fibre network to locally re-arrange itself along, and either side of, the valley fold line, to minimise local in-plane and out-of-plane bending stress, which permits the creation of stored energy as the trigger for subsequent deployment of the folded region; in a similar fashion to shape memory materials. In our system, the hydration triggered deployment is governed by (1) the softening of the bonded connection between the fibres and matrix, which triggers both (2) the release of the stored elastic energy to (minimise the bending stress gradient within the folded region), and (3) the swelling of the fibre network resulting in a geometric change through the thickness of the folded joint. To further clarify this point, Figure 4 *bottom row* illustrates the histology of fold creation in the handmade Sekishu 30 gsm paper. It can be observed that the fibres are re-arranged in such a way that they are closely aligned to the direction of fold (in effect, creating a 'living hinge'), thereby increasing the fibre volume fraction locally and increasing the bending stiffness of this region. The global fibre volume fraction (V_f) across the folded region remains constant, however at the foldline the V_f increases, whilst in the outside adjacent regions, the V_f is lower creating a zone of graded permeability (and for this particular application, the creation of a low resistance flow path for any penetrating liquid, see Figure 4 c). In our studies, this observation holds true for all the handmade paper types investigated.

4 Fold recovery upon drying

As noted in Section 2, natural dying of the specimens at room temperature resulted in some recovery of the initial folded configuration. The printer paper samples exhibited the greatest recovery (see Figure 5), whereas the recovery of the different handmade paper samples was not as pronounced. The potential for controllable reversible folding is of

considerable interest to the engineering community and therefore a series of experiments were undertaken to quantify the physical and structural reasons governing the angle 'recovered' upon drying.

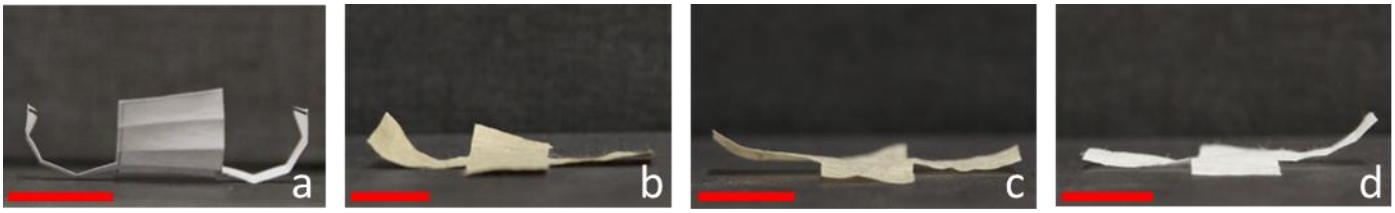

Figure 5: Shape recovery after deployment in a room temperature water bath and drying overnight (a) Printer paper 90 gsm; (b) Lokta 60 gsm; (c) Lokta 30 gsm and (d) Sekishu 30 gsm; Scale bar = 15mm

RECOVERY ANGLE

To determine the recovery angle, five samples of printer paper 90 gsm were deployed in a water bath, removed and then dried at room temperature overnight. Photographs from two directions (front view and side view) were taken to provide the means for calculating the recovery angle in each fold line for all four legs in each sample. ImageJ was used to calculate the angle at every fold locations. In stowed configuration the angle between each facelets forming the folds is 0°. Once fully deployed in water this angle becomes 180° as they lie flat on the water surface. The recovery fold angle, reported in Table 2, is determined from the difference between the fully deployed angle (180°) and the final resting position.

Table 2: Average recovery angle in printer paper for folds 1-6

for both directions		Average	Std dev
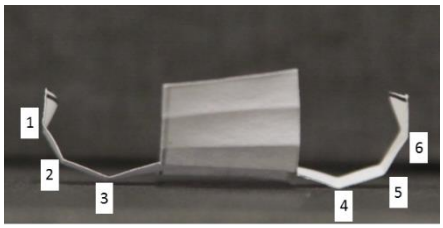	1	44.60	12.89
	2	42.83	8.67
	3	33.31	9.18
	4	39.05	14.66
	5	39.02	7.22
	6	44.82	11.30

One interesting observation concerns the repeatability of recovery angle in the same fold positions on different legs. For example, the outer folds in each leg (folds 1 and 6) and the middle folds in each leg (folds 2 and 5) have very similar values (see Table 2). Conversely, the inner folds (3 and 4) show the greatest discrepancy. It is speculated that this variation in 'actuator' response is a function of the bending moment associated with each fold (which will be greatest at fold 4, since the majority of the paper arm is outside the fold) and the action of water and surface tension 'pinning' the paper arm to bath substrate. Twisting of samples upon drying was also observed as shown in Figure 6. This presented a challenging scenario where the angle recovered would be different on either side of the fold line. In this study only one side was quantified. This type of minor twisting is believed to be the result of the fibre direction bias and the physical changes occurring in the fibres as they move through the drying cycle (namely, Hornification; discussed in Section 5). Comparatively, the handmade paper exhibited pronounced planar deformations (twisting and wrinkling) compared to more consistent twisting observed in the printer paper (Figure 6).

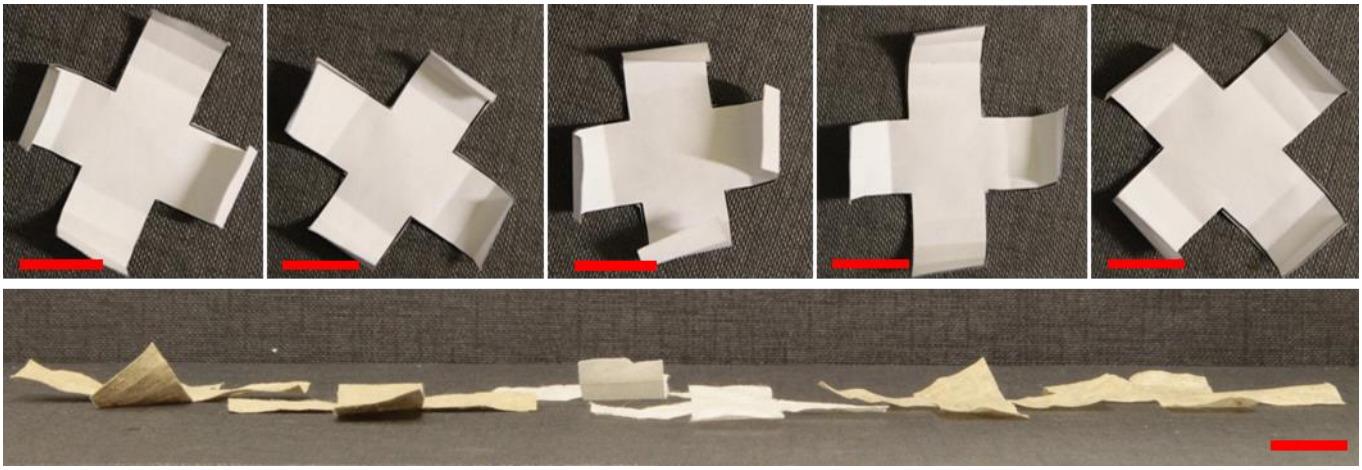

Figure 6: (Top) Twist observed in printer paper samples and (bottom): Planar deformations in handmade samples after drying dried after deployment. Scale bar = 15mm

To clarify the role of total fibre content (i.e. grammage) on fold angle recovery, a 90 gsm Lokta paper stack, comparable to the printer paper 90gsm, was created by combining three layers of Lokta 30 gsm paper. The layers were wetted out with water based cellulose adhesive Scolacell (Sodium Carboxymethyl cellulose) and consolidated together. Excess adhesive was rinsed off in water and dried under light pressure to minimise wrinkles. After deployment in water and drying, it was observed that the recovery in these Lokta 90 gsm samples were greater than the 30 gsm samples. Figure 7 shows the comparison of final recovered shape for printer paper 90 gsm, Lokta 90 gsm and Lokta 30 gsm. As expected, the role of fibre volume fraction significantly contributes towards the recovering the initial folded (stressed) configuration. It should also be noted, that fibre orientation, fibre-to-fibre connectivity and filler content, also play a significant role in fold recovery. In these studies, the role of the filler materials should not go unacknowledged; it provides a mechanism for substrate stabilisation once hydrated and subsequently helps minimise the wrinkles upon drying which contributes towards effective shape recovery in the printer paper specimens. Knowledge of fibre orientation, fibre-to-fibre connectivity (i.e. adhesion) and filler content, plus the stability of the host architecture when hydrated and the role of hornification, are essential in the design of any fibrous actuators based upon natural fibres.

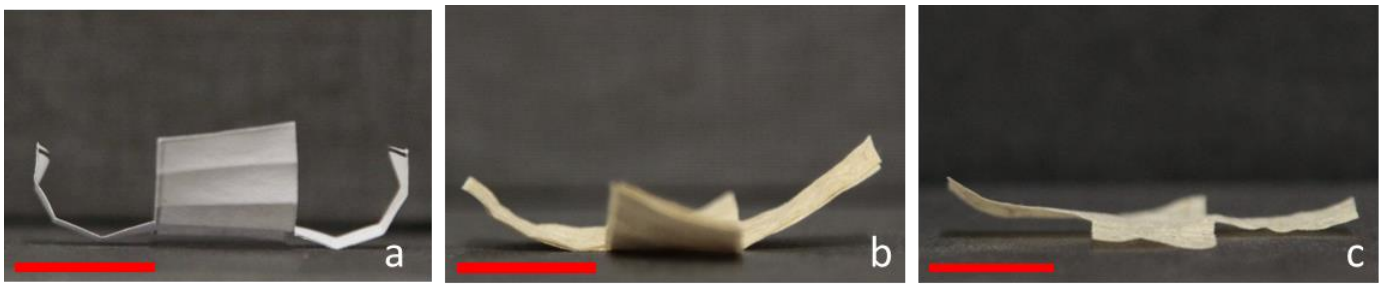

Figure 7: Recovery of sample architectures after deployment; (a) Printer paper 90 gsm, (b) Lokta 3x30 gsm and (c) Lokta 30 gsm. Scale bar = 15mm

5 Factors affecting deployment

The role of the architecture (shape, fold lines) and the deployment environment (nature and chemical composition of the medium) are all critical considerations when designing the active deployment of any morphing structure. In the previous section, consideration was given to specific variables, namely the role of paper weight (gsm) and stimuli. In this section, we extend the work and discussion to consider the role of the microstructure, changes in temperature, varying the surface tension (i.e. varying surfactant concentrations) and the role of dehydration for subsequent redeployment.

5.1 MICROSTRUCTURE

The local and global arrangement of the fibre architecture, and inherent nature of the porosity within the fibrous medium greatly affects the actuation response. Modifying the microstructure either by changing the fibre architecture or the porosity level through the application of fillers and coating can be used to manipulate water ingress and thus control the rate of deployment. Furthermore, as noted in Figure 5, upon the application of drying, the unfolded architecture tries to recover its original stowed shape. It is therefore conceivable that through the introduction of functional fillers that full recovery (back to the original shape) could be realised. Finally, and although not explored in this current study, the ability to selective position and align the cellulose fibres to create tuneable microstructures (through additive manufacturing/3D printing) where specific actuation pathways are printed within a global sheet, could be employed to realise sequential multi-stage deployment. Previous work by the authors [24] employing compliant polymeric membranes with locally reinforced regions based upon Kirigami principles has shown the potential of varying the strain potential for complex shape movement. Applying these principles in the formation of the fibrous medium, coupled with an active matrix, offers considerable potential for future morphing design concepts.

Hornification

The change in the fibrous architecture in the vicinity of the fold line along with functional fillers provides an inherent mechanism to promote fibrous 'spring-back' when the paper architecture is dried; this is shown in Figure 5. This phenomenon raises the possibility of creating a paper architecture with the potential of multiple deployment scenarios. During the course of this experimental investigation, it was noted that the second actuation of the same specimen was faster than the original deployment. The respective actuation times for a range of samples carried out at room temperature (25 °C) are presented in Table 3. The actuation time decreased with further actuation attempts and eventually stabilised. The data presented in Table 3 is the average of 5 samples tested. The standard deviation within each sample group has also decreased for subsequent actuations. It was also noted that the percentage change between subsequent actuations for specific samples were comparable to the group average.

Table 3: 1st and 2nd actuation times for different paper types at R.T (25 °C)

	Lokta 30 gsm	**Sekishu 30 gsm**	**Lokta 60 gsm**	**Printer paper 90 gsm**
1st (s)	25±4.47	37.6±11.84	132±9.80	313.1±152.4
2nd (s)	12±2.5	13±3.4	30±1.06	85±15
% change	-50.67%	-65.43%	-76.77%	-72.85%

This decrease in actuation time was attributed to water permanently affecting the local fibre architecture and the global microstructure of paper. Hornification is a technical term used in the paper industry to refer to the physical changes that fibres undergo upon recycling, i.e. wetting and drying [25]. Typically, hornification induces both a reduction in internal fibre volume and change in fibre aspect ratio. This shrinkage is irreversible upon the introduction of water. Figure 8 shows a SEM image of Sekishu fibres before and after hornification. It is clear that when the fibres shrink as a result of each wetting and drying processes, more free volume between the fibres is created, lowering the permeability of the system, thus allowing the fluid medium to penetrate faster and further. This rapid penetration, and subsequent breaking down the hydrogen bonds in the cellulose fibres, results in quicker actuation times.

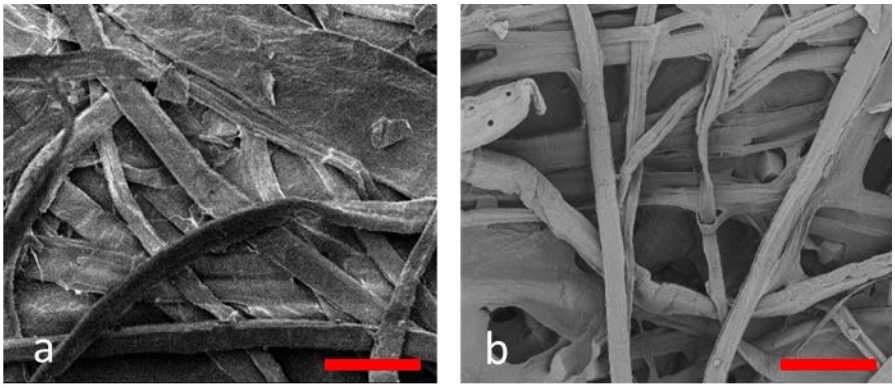

Dry fibres Fibres wetted and dried 5 times

Figure 8: SEM of dry fibres and fibres after hornification at 500x magnification; Scale bar 50µm

5.2 TEMPERATURE

Temperature of the actuating medium was found to have a significant effect on the actuation time. This is reasonable since the deployment actuation is a diffusion based absorption mechanism at the fluid-vapour interface. An increase in temperature results in an increased concentration of vapour-phase water molecules within the capillary formed by the fibrous network, i.e. the molecules at the interface have higher energy to escape the liquid phase. The partial vapour pressure increases with number of molecules in vapour state and facilitate diffusion transport of water molecules away from the liquid front into the paper substrate. The water molecules then condense and adsorb on to the surfaces of the fibres leading to a decrease in interfacial tension between the fibres and vapour phase, resulting in an increased wetting speed and low contact angle [26, 27].

The variation of 1st actuation time at different temperatures for the paper types investigated is illustrated in Figure 9 a. As expected, the actuation times were found to have decreased significantly at higher temperatures for all paper types. The polynomial decay in actuation times are indicative of the faster fluid transport into the substrate as a result of a dominant diffusion based absorption mechanism at higher temperatures [26, 28].

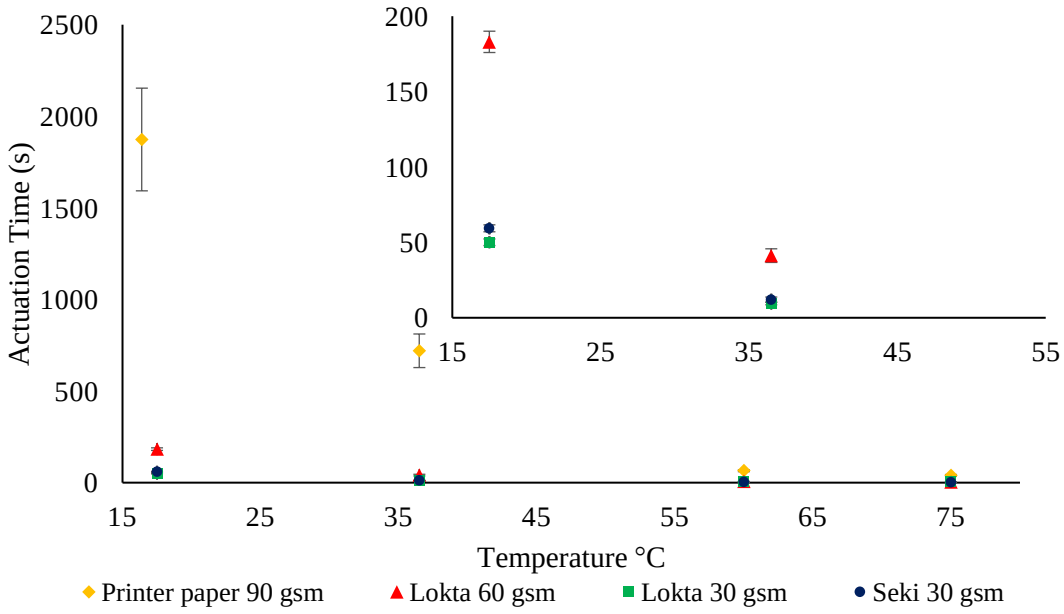

Figure 9 a: Variation of 1st actuation time at a range of temperatures. The insert image shows an enlarged snapshot of the fast actuation time of the handmade specimens below 55 ° C.

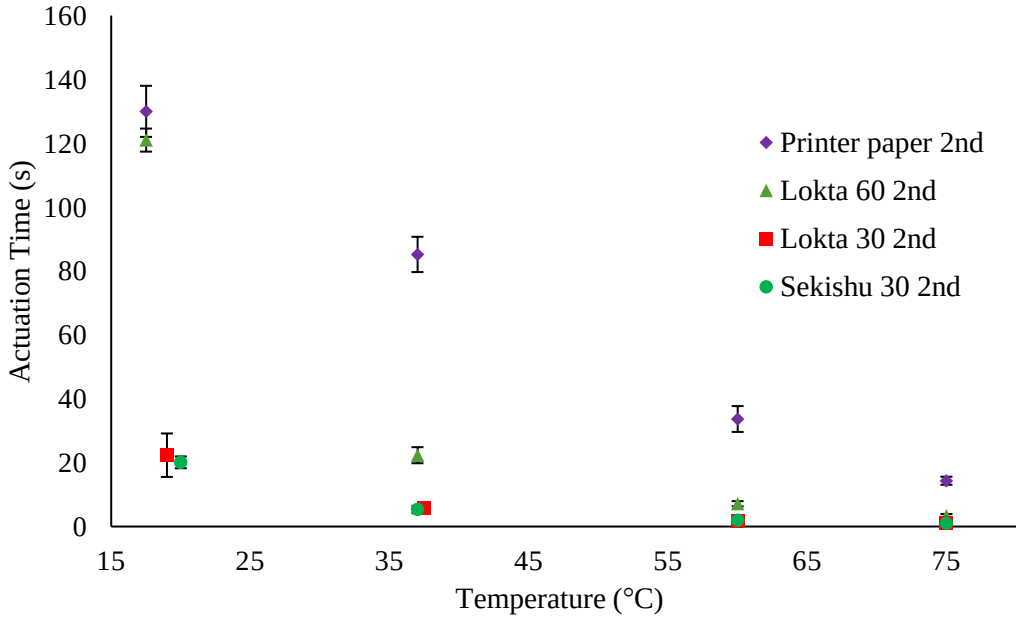

Figure 9 b: Variation of 2nd actuation times at a range of temperatures.

Figure 9 b shows the variation of 2nd actuation times of different paper types at a range of temperatures. A comparison with Figure 9 a shows that although all the handmade paper types follow a polynomial decay, the 2nd actuation times of printer paper does not decay at the same rate. The effects of hornification and filler content in the printer paper at higher temperatures is clearly evident from the response noted in Figure 9 b. The effect of microstructure (i.e. hornification) was also observed to have a smaller influence between 1st and 2nd actuation times at higher temperatures (> 50 °C). It can therefore be concluded that the response of these paper architectures is very sensitive to temperature variations in the actuating medium, and confirms that concentration gradient driven diffusion is the dominant mode of fluid transport in paper architectures.

5.3 SURFACTANTS

A faster deployment rate was observed for samples actuated in water containing varying surfactant concentrations. Sodium dodecyl sulfate (SDS) and Triton were added in concentrations of 1%, 0.1%, 0.01% and 0.001% by volume to the water bath. These surfactants differ in their nature as SDS is anionic and Trition is non-ionic. A reduction in surface tension was obtained for an increasing concentration of surfactants until the liquid surface was fully saturated with surfactant molecules. It can be seen from Figure 10 that there is minimal difference between the actuation times albeit the variation in surface tension values of the different surfactants used at given concentrations. However the decreasing trend observed in actuation times and surface tension suggests a positive correlation between the two. These results also implies that the actuation time is independent of surfactant type.

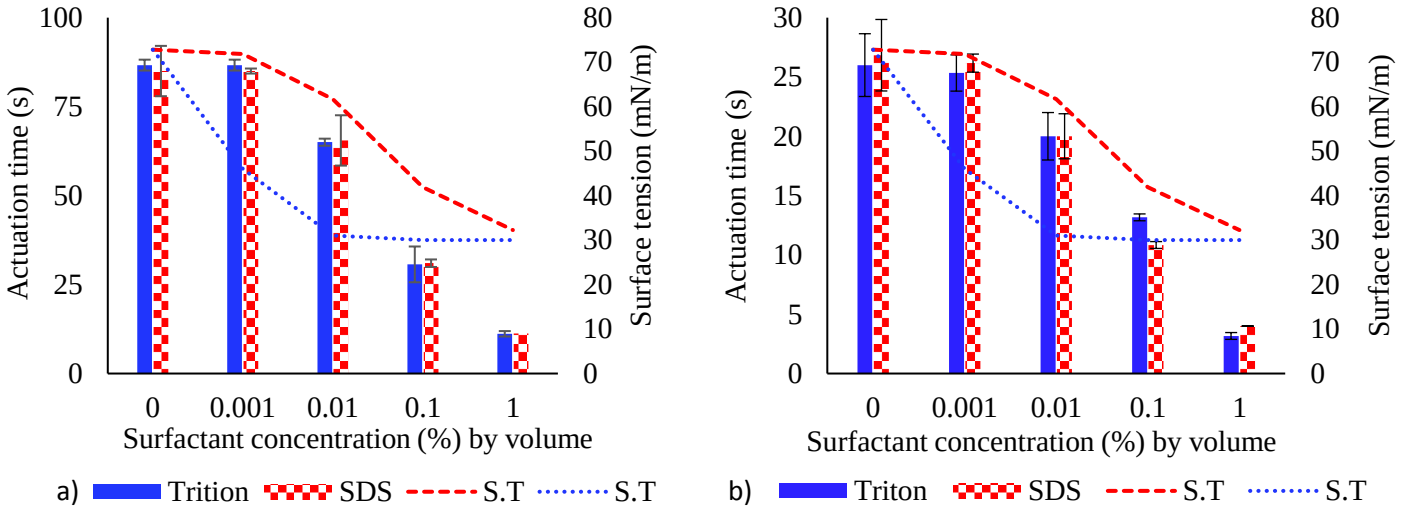

Figure 10: Variation of actuation time for corresponding % volume concentration of surfactants a) Printer paper 90gsm (2nd actuation) b) Lokta 30 gsm

6 Multi-layered composite systems

The lamina responsive form of the individual paper sheets offers the opportunity to create programmed morphing laminates by utilising different paper types, their orientation and stacking sequence. It was shown in Section 4 that higher fibre content achieved by means of layering individual sheets improves the fold recovery in paper architectures. Similar multi layered paper composites were prepared for this study using sodium carboxymethyl cellulose (CMC) as an adhesive inter layer. Lokta 30 gsm was chosen as the base unit for these systems as they had the highest rate of water absorption (Table 1) among the paper types considered. Lokta 60 gsm was also considered in order to study the influence of base unit 'size'. A key objective of this element of the study, was to ascertain the role of the adhesive bondline on (1) hornification of the cellulose fibres, (2) deployed activation times and (3) temperature. Table 4 shows the summary of the paper composites produced and their grammage.

Table 4: Summary of multi-layered paper composites

Configuration	**2 x 30 gsm**	**3 x 30 gsm**	**2 x 60 gsm**	**4 x 30 gsm**
Nominal	Lokta 60 gsm	Lokta 90 gsm	Lokta 120 gsm	Lokta 120 gsm
Measured gsm	72.6 ± 3.8	95.8 ± 0.2	105 ± 2.1	143.7 ± 5.5

As expected, the Na-CMC adhesive layer acts as a buffer slowing down water permeation in the through-thickness direction. Interestingly, the presence of CMC layer promoted a different substrate flow pathway, as indicated in Figure 11. In the absence of CMC layer, water uniformly saturates the substrate in the through thickness direction (Figure 11 a and b), whereas in the Lokta composite saturation proceeds from the free-edge boundary to the core (Figure 11 c) as its offers least resistance. Controlling the permeability of the different layers offers the potential for sequenced in-plane and out-of-plane deployment.

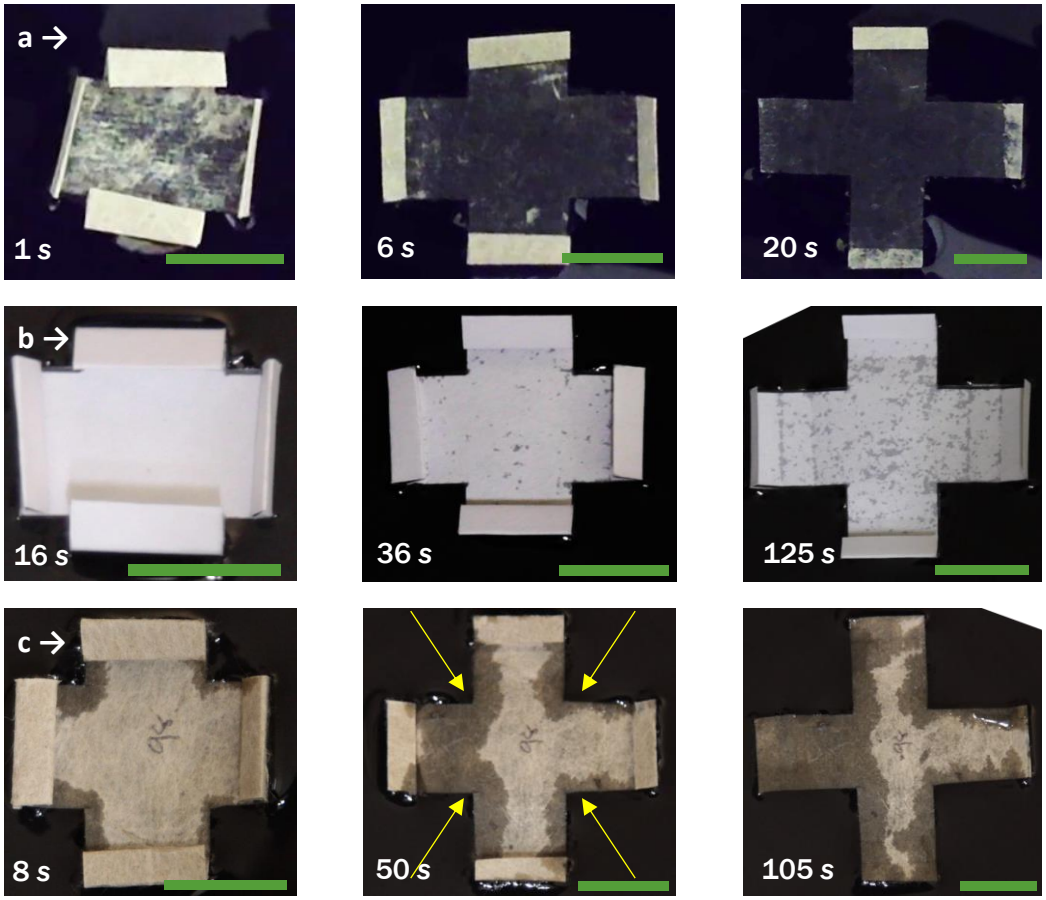

Figure 11: Flow characteristics: (a) Lokta 30 gsm; (b) Printer paper 90 gsm; (c) Lokta 3 x 30 composite. Scale bar: 15 mm

Similar to the individual lamina sheet studies, the first and second actuation times at room temperature (24 °C) for the different paper composite configurations were characterised; these results are reported in Figure 12. Upon closer examination, it can be seen that Lokta 2 x 30 gsm and Lokta 4 x 30 gsm samples actuated faster than the corresponding Lokta 60 gsm and Lokta 2 x 60 gsm systems. For our chosen materials, this clearly suggests that lighter base lamina assembled to create a target gsm is more efficient for morphing than the heaver base units, despite the introduction of additional adhesive layers inhibiting through thickness water ingress. Unfortunately, the presence of adhesive layers did result in a non-uniform distributed water content across paper composites (even at full deployment, see Figure 11 c), thereby resulting in non-uniform hornification effect. Clearly, this poses a significant challenge to developing a repeatable paper based composite actuator using this strategy.

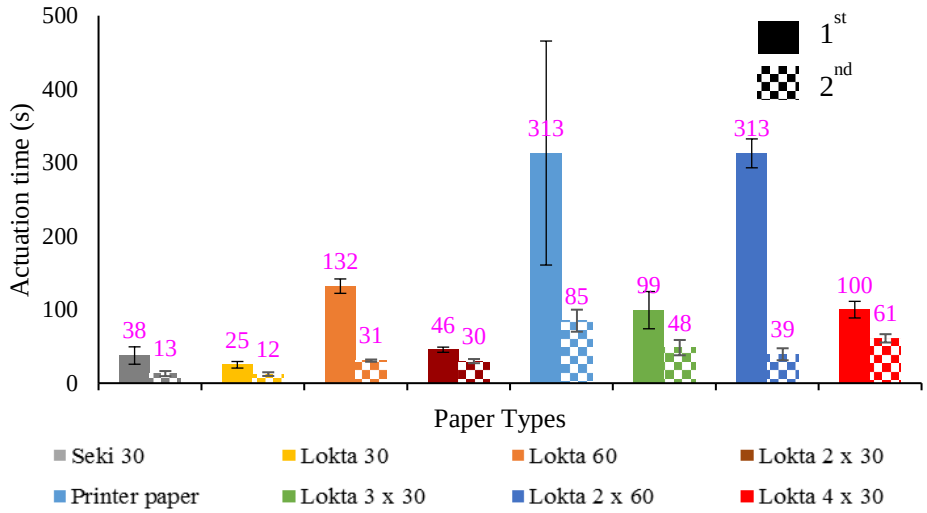

Figure 12: Comparison of first and second actuation times for different paper types (The average and standed deviation is of 5 specimens)

7 Discussion

The principle component of paper fibre is cellulose. Hydrogen bonding in cellulose chains forms fibrils which further associate to form the fibres; these fibres form an interwoven network resulting in the hierarchical structure of paper [29]. Cellulose molecules have a crystalline and amorphous region where the hydrogen bonding within the crystalline part is very stable compared to the amorphous region [30]. The introduction of water or moisture into cellulose has a plasticizing effect on the amorphous region by weakening or 'relaxing' the inter-fibre hydrogen bonding. Intercalating water molecules forming hydrogen bonds between fibrils, along with water retained in inter and intra fibre pores, results in swelling of the fibres, in effect causing the paper to behave like a bi-layer film as the water front propagates through the thickness direction. The resultant stress relaxation at the folds promotes fold deployment, since it is no longer capable of supporting the bending stress. The fluid transport mechanism was found to be a combination of diffusion and capillary effect through inter-intra fibre pores; the diffusion based mechanism was found to be even more prominent at higher temperatures due to increased partial vapour pressure.

The effect of porosity and paper weight was very clearly demonstrated in our deployment experiments. Apart from influencing the actuation times, the microstructure also influenced the shape recovery. Physical changes in microstructure (both natural and intentional) can be utilised by the designer to program a desired behaviour in a synthetic analogue of the cellulose actuators considered in this study.

The role of different activating mediums was considered. The motivation to try glycerol was due to its similar surface tension value to that of water and the number of OH groups present in the molecule for hydrogen bonding. It is believed that Glycerol was capable of interacting with the hydrogen bonding within the cellulose architecture resulting in the swelling and deployment of the fold. In our experiments this did occur for all the paper types, albeit over significantly longer time periods than the samples triggered by water. It should be noted that the printer paper and Lokta 60gsm did not open over the same time period and it is speculated that the filler content and higher fibre V_f inhibited the ingression of the Glycerol. As the experiment was left for a significantly longer time period (12 hrs); deployment of the fold lines did occur. However, it is clear that the formation and breakdown of hydrogen bonds is critical for deployment in these architectures. The role and influence of surfactants was also investigated to ascertain whether this had any effect on the mass migration of the water molecules into the cellulose architecture. Interestingly, the addition of surfactants (whether anionic or non-ionic) does have a decreasing effect on the actuation time of the samples tested. However, the actuation time at a given surfactant concentration despite the difference in surface tension was found to be comparable. Therefore, it is postulated that the decreasing effect is believed to be a function of the number of surfactant molecules and their physical arrangement at the water surface-paper boundary, and the control this imparts on the rate of fluid transport into the substrate, as opposed to the reduction of surface tension which is the primary consequence of surfactant addition.

Actuation of multi-layered paper composites revealed the significance of base unit in achieving fast actuation times. Previous experiments with homogenous lamina sheet samples indicated a proportional relationship with paper weight (grammage) and activation times; however, our studies show this trend is not translated to multi-layered composite architectures. Architectures with smaller base units actuated faster despite being heavier in grammage. It can be concluded that layering is an efficient way of promoting water transport into the substrate resulting in swelling and actuation. However, such a layered system is somewhat limited in the context of repeatable actuator due to uneven hornification effects in the substrate. The samples were removed from water surface once full actuation was achieved regardless of whether full saturation had occurred. Such a procedure will result in non-uniform hornification across the samples. This resulted in a large standard deviation in 2nd actuation times especially at higher temperatures. The effect of temperature on the adhesive layer and water absorption properties is an area which requires further investigation.

8 Conclusions

The study has investigated the deployment of a 'model' folded paper architecture, using the medium of water as the stimulus for self-actuation. Our work has been inspired by the passive nastic movements exhibited by biological systems (such as pinecone scales and wheat awns), which achieve complex deployment with cellulose fibres. Our goal has been to capture the 'design rules' for active morphing in a 'natural' fibrous system for translation into a synthetic fibrous counterpart.

To understand our model system, we have characterised different cellulose architectures and stimuli mechanisms to quantify their role and influence on folded deployment. We have shown how the random cellulose architecture aligns around the mountain folds triggering neighbouring regions of lower fibrous volume fraction, which permit and promote moisture ingress to weaken/'relax' the cellulose inter-fibre hydrogen bonding, allowing the locked-in strain to trigger deployment. This work clearly shows that by controlling the cellulose architecture which in turn controls the local fluid ingress, permits the design of fibrous structures for programmable deployment. Scalability is critical for successfully adapting a system across different length scales. Layering individual lamina sheets into a typical composite structure has been explored. This approach illustrated the significance of the base unit configuration for controlled deployment. Some caveats to repeatable actuations based on existing procedures were identified and suggestions to mitigate those limitations were also presented. Besides actuation time, a key parameter in the characterisation of rotational actuator system is stall torque which is defined as the limiting torque applied to the actuator to prevent deployment, i.e. a blocking force. With regard to the model actuator investigated in this study, this parameter can be measured for a single fold for a specific type of paper and/configurations. This would give an insight into the relationship between force/moment output of the actuator and material properties. Since the blocking force is likely to be very small, and governed by the response of the fibrous architecture to the hydration and dehydration environment, in both the folded region and along the 'hinge' arm, a block force experiment recording the tip displacement within an environmental chamber would be required which eliminates any external friction or capillary forces. Presently, the authors are exploring and devising an experimental procedure to determine both these parameters for different paper architectures; this will be reported in a subsequent publication.

In terms of a design philosophy, clearly the introduction of fibre pre-strain in the folded region; functionally graded fibre architecture between the folds; a matrix material which offers programmable adhesion; coupled with an internal porous architecture which permits the 'stimulus' the opportunity to reach and activate/deactivate the 'fibre-matrix' interface, would be ideal. The current state-of-the-art capability in synthetic fibrous and matrix materials can currently resolve most of these design requirements, e.g. the ability to pre-strain synthetic fibres is possible; similarly creating functionally graded architectures; creating an internal porous architecture is equally viable. However, and perhaps most critically, it is the ability to activate and deactivate the fibre-matrix interfacial properties on demand which is needed. Addressing and solving this requirement is the key technical challenge for any future fibrous 4D material for programmed complex 3-dimension shape change.

9 Acknowledgements

This work was supported by the Engineering and Physical Sciences Research Council through the EPSRC Centre for Doctoral Training in Advanced Composites for Innovation and Science [grant number EP/G036772/1] and for funding RST's fellowship and research under EPSRC 'Engineering Fellowships for Growth' [grant number EP/M002489/1]

10 References

[1] Y. Liu, J. K. Boyles, J. Genzer, and M. D. Dickey, "Self-folding of polymer sheets using local light absorption," *Soft Matter*, vol. 8, no. 6, p. 1764, 2012.
[2] Q. Ge, C. K. Dunn, H. J. Qi, and M. L. Dunn, "Active origami by 4D printing," *Smart Mater. Struct.*, vol. 23, no. 9, pp. 1–15, Sep. 2014.
[3] A. R. Studart and R. M. Erb, "Bioinspired materials that self-shape through programmed microstructures," *Soft Matter*, vol. 10, no. 9, pp. 1284–1294, Mar. 2014.
[4] L. Ionov, "Soft microorigami: self-folding polymer films," *Soft Matter*, vol. 7, no. 15, p. 6786, 2011.
[5] Q. Zhao, J. W. C. Dunlop, X. Qiu, F. Huang, Z. Zhang, J. Heyda, J. Dzubiella, M. Antonietti, and J. Yuan, "An instant multi-responsive porous polymer actuator driven by solvent molecule sorption," *Nat. Commun.*, vol. 5, p. 4293, Jan. 2014.
[6] R. M. Erb, J. S. Sander, R. Grisch, and A. R. Studart, "Self-shaping composites with programmable bioinspired microstructures," *Nat. Commun.*, vol. 4, p. 1712, Jan. 2013.
[7] R. Yoshida and T. Okano, "Biomedical Applications of Hydrogels Handbook," pp. 19–44, 2010.
[8] E. Palleau, D. Morales, M. D. Dickey, and O. D. Velev, "Reversible patterning and actuation of hydrogels by electrically assisted ionoprinting," *Nat. Commun.*, vol. 4, p. 2257, 2013.
[9] G. Stoychev, S. Zakharchenko, S. Turcaud, J. W. C. Dunlop, and L. Ionov, "Shape-programmed folding of stimuli-responsive polymer bilayers," *ACS Nano*, vol. 6, no. 5, pp. 3925–3934, 2012.
[10] S. Timoshenko, "Analysis of Bi-Metal Thermostats," *J. Opt. Soc. Am.*, vol. 11, no. 3, pp. 233–255, Sep. 1925.
[11] S. Alben, "Bending of bilayers with general initial shapes," *arXiv*, p. 1110.1007v1, 2011.
[12] E. Reyssat and L. Mahadevan, "Hygromorphs: from pine cones to biomimetic bilayers.," *J. R. Soc. Interface*, vol. 6, no. 39, pp. 951–957, 2009.
[13] S. Reichert, A. Menges, and D. Correa, "Meteorosensitive architecture: Biomimetic building skins based on materially embedded and hygroscopically enabled responsiveness," *Comput. Des.*, vol. 60, pp. 50–69, 2015.
[14] E. Cliquet, "Flotilla." [Online]. Available: http://ordigami.net/flotilla.php.
[15] I. Burgert and P. Fratzl, "Actuation systems in plants as prototypes for bioinspired devices.," *Philos. Trans. A. Math. Phys. Eng. Sci.*, vol. 367, no. 1893, pp. 1541–57, Apr. 2009.
[16] R. Elbaum, L. Zaltzman, I. Burgert, and P. Fratzl, "The role of wheat awns in the seed dispersal unit.," *Science*, vol. 316, no. 5826, pp. 884–886, 2007.
[17] Q. Ibrîm, T. M. Peakman, M. Biddle, C. Dawson, J. F. V Vincent, and A.-M. Rocca, "How pine cones open," *Nat.*, vol. 390, no. 6661, p. 668, 1997.
[18] J. Agbenyega, "Nanostructured origami," *Mater. Today*, vol. 12, no. 4, p. 12, 2009.
[19] Z. You, "A novel foldable stent graft," 2004.
[20] "Deployable Mast." [Online]. Available: http://www.nustar.caltech.edu/page/mast. [Accessed: 17-Aug-2015].
[21] J. Grönfors, "Use of fillers in paper and paperboard grades," 2010.
[22] Australian Maritime Safety Authority, "Viscosity of oils and other natural products." [Online]. Available: https://www.amsa.gov.au/environment/maritime-environmental-emergencies/national-plan/Supporting-Documents/viscosity-of-oils/index.asp.
[23] M. A. MacGregor, "Some impacts of paper making on paper structure," *Pap. Technol.*, vol. 42, no. 3, pp. 30–44, 2001.
[24] S. Daynes, R. S. Trask, and P. M. Weaver, "Bio-inspired structural bistability employing elastomeric origami for morphing applications," *Smart Mater. Struct.*, vol. 23, no. 12, p. 125011, 2014.
[25] J. L. Minor, "Hornification -Its origin and meaning," *Progrress Pap. Recycl.*, vol. 3, no. 2, pp. 93–95, 1994.
[26] J. Songok, P. Salminen, and M. Toivakka, "Temperature effects on dynamic water absorption into paper," *J. Colloid Interface Sci.*, vol. 418, pp. 373–377, Mar. 2014.
[27] J. B. Rosenholm, "Wetting of Surfaces and Interfaces: A Conceptual Equilibrium Thermodynamic Approach,"

in *Colloid Stability: The Role of Surface Forces - Part II*, vol. 2, Wiley-VCH Verlag GmbH & Co. KGaA, 2011, pp. 1–83.
[28] E. Reyssat and L. Mahadevan, "How wet paper curls," *EPL (Europhysics Lett.*, vol. 93, no. 5, p. 54001, Mar. 2011.
[29] M. Seery, "Saving paper," *Educ. Chem.*, no. March, pp. 22–25, 2013.
[30] C. Zhou and Q. Wu, "Recent development in applications of cellulose nanocrystals for advanced polymer-based nanocomposites by novel fabrication strategies," *Nanocrystals – Synth. Charact. Appl. Prop.*, pp. 103–120, 2012.